Vibronic spectra of mixed Frenkel and charge transfer excitons

I. J. Lalov and I. Zhelyazkov
Faculty of Physics, Sofia University, BG-1164 Sofia, Bulgaria
(Received 30 January 2006; revised manuscript received 24 April 2006; published 6 July 2006)

The excitonic and vibronic spectra of a molecular chain and of a crystal of *NN'*-dimetyl 3,4,9,10-perylene tetracarboxylic diimide (MePTCDI) are studied in the case when: (i) a Frenkel exciton (FE) and charge transfer excitons (CTEs) mix strongly; and (ii) two mechanisms of coupling between these mixed excitons and intramolecular vibrations, notably linear and quadratic coupling, are acting. Using a convenient canonical transformation and the Green function method, we calculate the linear optical susceptibility: (a) in the exciton region taking into account the contribution of the transition dipoles of FE; and (b) in one-phonon vibronic regime. The spectra of linear absorption in the excitonic and vibronic regions have been calculated introducing the exciton parameters of MePTCDI. These spectra exhibit: (i) a relative separation of vibronics of FE and CTEs; (ii) a stronger impact of the linear coupling on the intensity of the excitonic and vibronic spectra; and (iii) the appearance of a spectral doublet of vibronics of the CTEs—its splitting depends on the parameters of linear and quadratic exciton–phonon coupling in the neutral excited molecule and ions. Moreover, in the case of weak linear exciton–phonon coupling the vibronic line of FE, being wide and flat, lies in many-particle continuum while in the case of intermediate and strong linear coupling the linear absorption is dominated by the bound exciton–phonon states and their narrow Lorentzian maxima depend strongly on the quadratic coupling.

DOI: 10.1103/PhysRevB.74.035403 PACS number(s): 78.40.Me, 73.20.Mf

I. INTRODUCTION

In the previous study,[1] we investigated the excitonic and vibronic spectra of MePTCDI and 3,4,9,10-perylene tetracarboxylic dianhydride (PTCDA) crystals in the case of mixing of Frenkel excitons (FEs) and the lowest charge transfer excitons (CTEs). The features of the model which allow us to find an exact solution to the many-particle problem with complicated FE–CTEs–phonon coupling are as follows: (i) the molecules in these crystals are ordered in quasi-one-dimensional stacks; (ii) the lowest excitonic excitation appears as a result of mixing of a FE and first CTEs and that excitation is separated from the second CTEs state; (iii) the intramolecular vibration preserves its properties (frequency) in the nonexcited and excited molecule as well as in the ion; and (iv) the transfer integrals of FE, the hole, and the electron between neighbor molecules have relatively small values compared with the vibrational frequency.

In this paper, we investigate again the linear absorption and preserve the main features (i)–(iv) of the above-mentioned model [with a possible exception of item (iii)] but we expand it in several directions, namely: (a) we consider two mechanisms of exciton–phonon coupling—the linear coupling (see Refs. 1–4) and the quadratic coupling which causes changes of the vibrational frequency in the molecule with FE[5,6] and in the ionized molecule;[7] and (b) although using data for the mobility of FE and CTEs in a MePTCDI crystal, we do hope to find other substances in which the model of vibronics for the case of linear and quadratic exciton–phonon coupling may be applied. Thus we calculate the excitonic absorption in the case of more significant change of the vibrational frequency in the excited molecule.

The organization of this paper is as follows: in Sec. II we find the vibronic Hamiltonian in the one-dimensional chain in the case of linear and quadratic exciton (FE and CTEs)–phonon coupling. We use the canonical transformation which generalizes the transformation in the case of vibronics of pure FE.[5,6] Section III contains the main analytical results on the linear optical susceptibility of the one-dimensional chain in excitonic and vibronic regions. Section IV deals with the calculations of the linear absorption spectra in the same frequency regions using the exciton data for the MePTCDI crystal. We also study the absorption in a more hypothetical case of a significant change of the vibrational frequency in the excited molecule. Section V contains conclusions on the manifestation of excitons and their vibronics in the linear processes. Two Appendices are devoted to some details of the canonical transformation.

II. FE–CTES–PHONON HAMILTONIAN

As in other papers on excitonic and vibronic spectra in PTCDA and MePTCDI crystals[1,3,4,8,9] we consider excitations in a linear chain of regularly ordered molecules $n=1,2,\ldots,N$. It corresponds to stacks in which the molecules are situated closer than their neighbors in the perpendicular plane.

The initial Hamiltonian consists of three parts:

$$\hat{H}=\hat{H}_{\mathrm{ex}}+\hat{H}_{\mathrm{phon}}+\hat{H}_{\mathrm{ex-phon}}, \tag{1}$$

where $\hat{H}_{\mathrm{ex}}$ is the well-known Hamiltonian of mixed FE and CTEs:[1,8,9]

$$\begin{aligned}\hat{H}_{\mathrm{ex}}=&\sum_{n}E'_{\mathrm{F}}B_n^{+}B_n+\sum_{n,n'}L'(\delta_{n',n+1}+\delta_{n',n-1})B_n^{+}B_{n'}\\&+\sum_{n,\sigma=1,2}E'_{\mathrm{c}}C_{n\sigma}^{+}C_{n\sigma}+\sum_{n,\sigma}\varepsilon'_{\mathrm{e}}[B_n^{+}C_{n\sigma}+\mathrm{H.c.}]\\&+\sum_{n}\varepsilon'_{\mathrm{h}}[B_n^{+}C_{n+1,2}+B_n^{+}C_{n-1,1}+\mathrm{H.c.}].\end{aligned} \tag{2}$$

Here, B_n (B_n^+) is the annihilation (creation) operator of Frenkel exciton on the molecule n, E_F' and L' are correspondingly the excitation energy of FE and its transfer integral between the neighbor molecules n and $n\pm1$, $C_{n\sigma}$ is the annihilation operator of CTEs whose hole is based on site n and the electron is located on site $n+1$ (CTE $\sigma=1$) or on site $n-1$ (CTE $\sigma=2$), E_c' is the excitation energy of CTEs. We consider the degenerate case $E_{c1}'=E_{c2}'=E_c'$ that is a consequence of the inversion symmetry of the chain and neglect the transfer of CTEs as a whole. The quantities ε_e' and ε_h' represent charge transfer integrals of the electron and the hole from the molecule n with a Frenkel exciton to its neighbors.

We consider the vibronic spectra with one intramolecular vibrational mode only and express the phonon's part $\hat{H}_{\text{phon}}$ as follows:

$$\hat{H}_{\text{phon}} = \sum_n \hbar\,\omega_0 a_n^+ a_n, \tag{3}$$

where ω_0 is the vibrational frequency in the nonexcited molecule and a_n is the annihilation operator of one vibrational quantum on molecule n.

The operator of exciton–phonon coupling $\hat{H}_{\text{ex–phon}}$ contains linear and quadratic terms of the dimensionless phonon normal coordinate X_n:

$$X_n = a_n + a_n^+. \tag{4}$$

That operator can be split into three parts:

$$\hat{H}_{\text{ex–phon}}^{(1)} = \sum_n \hbar\,\omega_0 B_n^+ B_n [dX_n + eX_n^2], \tag{5a}$$

$$\hat{H}_{\text{ex–phon}}^{(2)} = \sum_{n,\sigma=1,2} \hbar\,\omega_0 C_{n\sigma}^+ C_{n\sigma} [d^+ X_n + e^+ X_n^2], \tag{5b}$$

$$\hat{H}_{\text{ex–phon}}^{(3)} = \sum_{n,\sigma=1,2} \hbar\,\omega_0 C_{n\sigma}^+ C_{n\sigma} [d^- X_{n+\sigma_1} + e^- X_{n+\sigma_1}^2], \tag{5c}$$

where

$$\sigma_1 = +1 \text{ if } \sigma = 1; \quad \sigma_1 = -1 \text{ for } \sigma = 2.$$

The dimensionless quantities d, d^+, d^- describe the displacement of the nuclei's equilibrium positions in a molecule with FE, in a positive (d^+) and a negative (d^-) ion, respectively. Quantities e, e^+, e^- are introduced to describe the changes of the parabolic potential of vibrating nuclei in an electronically excited molecule and they express the quadratic exciton–phonon coupling in the same molecule and ions.

The operator $\hat{H}_{\text{ex–phon}}$ can be eliminated by using the following canonical transformation:[5,7]

$$\hat{H}_1 = e^Q \hat{H} e^{-Q}, \tag{6}$$

where

$$\begin{aligned} Q = \sum_{n,\sigma} \{ & \tau B_n^+ B_n [a_n^2 - (a_n^+)^2 + \theta(a_n - a_n^+)] \\ & + \tau_1 C_{n\sigma}^+ C_{n\sigma} [a_n^2 - (a_n^+)^2 + \theta_1 (a_n - a_n^+)] \\ & + \tau_2 C_{n\sigma}^+ C_{n\sigma} [a_{n+\sigma_1}^2 - (a_{n+\sigma_1}^+)^2 + \theta_2 (a_{n+\sigma_1} - a_{n+\sigma_1}^+)] \}. \end{aligned} \tag{7}$$

We treat here a linear problem with one exciton. Thus the eigenvalues of the operators $B_n^+ B_n$ and $C_{n\sigma}^+ C_{n\sigma}$ are 0 or 1 and the following relations hold:

$$\begin{aligned} B_n^+ B_n B_{n_1}^+ B_{n_1} &= B_n^+ B_n \delta_{nn_1}, \\ C_{n\sigma}^+ C_{n\sigma} C_{n_1\sigma'}^+ C_{n_1\sigma'} &= C_{n\sigma}^+ C_{n\sigma} \delta_{nn_1} \delta_{\sigma\sigma'}, \\ B_n^+ B_n C_{n_1\sigma}^+ C_{n_1\sigma} &= 0, \end{aligned} \tag{8}$$

$$\sum_{n,\sigma} [B_n^+ B_n + C_{n\sigma}^+ C_{n\sigma}] = 1. \tag{9}$$

We eliminate terms (5) of the linear and quadratic exciton–phonon coupling by applying transformation (6) with the following values of the quantities τ, τ_1, τ_2, θ, θ_1, θ_2 [on using relations (8) and (9)]:

$$e^{-4\tau} = \sqrt{1+4e}, \quad e^{-4\tau_1} = \sqrt{1+4e^+}, \quad e^{-4\tau_2} = \sqrt{1+4e^-}; \tag{10}$$

$$\begin{aligned} \theta &= -\frac{2d}{(1+4e)[\exp(2\tau)-1]}, \\ \theta_1 &= -\frac{2d^+}{(1+4e^+)[\exp(2\tau_1)-1]}, \\ \theta_2 &= -\frac{2d^-}{(1+4e^-)[\exp(2\tau_2)-1]}. \end{aligned} \tag{11}$$

Using relations (6)–(11) we obtain the following Hamiltonian (for details see Appendix B):

$$\begin{aligned} \hat{H}_1 = & \sum_n E_F B_n^+ B_n + \sum_{n,\sigma} E_c C_{n\sigma}^+ C_{n\sigma} + \sum_n \hbar\,\omega_0 a_n^+ a_n \\ & + \sum_n \hbar\,\Delta\omega B_n^+ B_n a_n^+ a_n + \sum_{n,\sigma} \hbar\,\Delta\omega^+ C_{n\sigma}^+ C_{n\sigma} a_n^+ a_n \\ & + \sum_{n,\sigma} \hbar\,\Delta\omega^- C_{n\sigma}^+ C_{n\sigma} a_{n+\sigma_1}^+ a_{n+\sigma_1} + \hat{H}_{\text{int}} \end{aligned} \tag{12}$$

with

$$\begin{aligned} \hat{H}_{\text{int}} = & \sum_{n,n'} L'(\delta_{n',n+1} + \delta_{n',n-1}) V_{n'}^+ V_n + \sum_{n,\sigma} \varepsilon_e' [V_n^+ U_{n\sigma} + \text{H.c.}] \\ & + \sum_n \varepsilon_h' [V_n^+ U_{n+1,2} + V_n^+ U_{n-1,1} + \text{H.c.}], \end{aligned} \tag{13}$$

where

$$E_F = E_F' - \frac{d^2}{1+4e}\hbar\,\omega_0 + \frac{\hbar}{2}\Delta\omega, \tag{14a}$$

$$E_c = E_c' - \left(\frac{(d^+)^2}{1+4e^+} + \frac{(d^-)^2}{1+4e^-} \right) \hbar\omega_0 + \frac{\hbar}{2}(\Delta\omega^+ + \Delta\omega^-), \tag{14b}$$

$$\Delta\omega = \omega_0(\sqrt{1+4e} - 1), \quad \Delta\omega^{\pm} = \omega_0(\sqrt{1+4e^{\pm}} - 1), \tag{14c}$$

$$V_n = e^Q B_n e^{-Q}, \tag{14d}$$

$$U_{n\sigma} = e^Q C_{n\sigma} e^{-Q}. \tag{14e}$$

Relations (10)–(14) are exact and we can study the vibronics in the case of simultaneous action of the linear and quadratic coupling. Further calculations have been performed by making the following assumptions.

(1) The parameters of the exciton–phonon coupling in the positive and negative ions have been taken to be equal, i.e.,

$$d^+ = d^- \quad \text{and} \quad e^+ = e^- \tag{15}$$

(but the parameters of the exciton–phonon coupling in the excited neutral molecule being different, $d^+ \neq d$, $e^+ \neq e$). This is a usual approximation in the studies of vibronics of the MePTCDI and PTCDA crystals[3,4] and it is not a principal limitation.

(2) We suppose the energy $\hbar\omega_0$ of the vibrational quantum to be larger than the exciton transfer integrals,

$$\hbar\omega_0 > |L'|, |\varepsilon_e'|, |\varepsilon_h'|. \tag{16}$$

Inequality (16) is similar to the basic assumption $\hbar\omega_0 > |L'|$ of the so-called dynamical theory of the vibronics of FE. According to that theory (see Ref. 5) all terms in the Hamiltonian which do not conserve the number of phonons can be eliminated. Following the same approach, we preserve in operator (13) only those terms which commutate with the operator of the total phonon numbers

$$\hat{N}_{\text{phon}} = \sum_n a_n^+ a_n, \tag{17}$$

and find the following expression for the exciton mobility part (13) of the Hamiltonian (see the Appendix B):

$$\begin{aligned} \hat{H}_{\text{int}} = & \sum_{n,n'} L(\delta_{n',n+1} + \delta_{n',n-1}) B_{n'}^+ B_n \\ & \times \{1 + \eta_1 [a_{n'}^+ a_n e^{2\tau} - (a_n^+ a_{n'} + a_n^+ a_n) + a_n^+ a_{n'} e^{-2\tau}]\} \\ & + \sum_{n,\sigma} \varepsilon_e \{B_n^+ C_{n\sigma} [1 - \eta_4 a_n^+ a_n + \eta_3 (a_n^+ a_{n+\sigma_1} + a_{n+\sigma_1}^+ a_n e^{-2\tau}) \\ & - \eta_2 a_{n+\sigma_1}^+ a_{n+\sigma_1}] + \text{H.c.}\} + \sum_{n,\sigma} \varepsilon_h \{B_n^+ C_{n-\sigma_1,\sigma} \\ & \times [1 - \eta_4 a_n^+ a_n + \eta_3 (a_n^+ a_{n-\sigma_1} + a_{n-\sigma_1}^+ a_n e^{-2\tau}) \\ & - \eta_2 a_{n-\sigma_1}^+ a_{n-\sigma_1}] + \text{H.c.}\}, \end{aligned} \tag{18}$$

where

$$L = L' \exp(2\delta_1), \quad \varepsilon_e = \varepsilon_e' \exp W, \quad \varepsilon_h = \varepsilon_h' \exp W, \tag{19}$$

$$\eta_1 = d_1^2 \exp(-2\tau)/\cosh^2(2\tau), \tag{20}$$

$$\eta_2 = d_2^2 \exp(-2\tau_1)/\cosh^2(2\tau_1),$$

$$\eta_3 = (d_1 - d_2) d_2 \exp(-2\tau_1)/\{\cosh[2(\tau - \tau_1)]\cosh(2\tau_1)\}, \tag{21}$$

$$\eta_4 = (d_1 - d_2)^2 \exp[-2(\tau + \tau_1)]/\cosh^2[2(\tau - \tau_1)], \tag{22}$$

$$d_1 = d/(1+4e), \quad d_2 = d^+/(1+4e^+), \tag{23}$$

$$\exp(2\delta_1) = \exp\{-2d_1^2/[1+\exp(4\tau)]\}/\cosh(2\tau), \tag{24}$$

$$\begin{aligned} W = & -\frac{1}{2} \ln\{\cosh[2(\tau - \tau_1)]\cosh(2\tau_1)\} - (d_1 - d_2)^2 \\ & \times \exp(-4\tau_1)/\{1 + \exp[4(\tau - \tau_1)]\} - d_2^2/[1 + \exp(4\tau_1)]. \end{aligned} \tag{25}$$

The reduction of exciton mobility part (13) of the Hamiltonian to the operator (18) allows us to find out exact solutions for the vibronic spectra and for the linear optical susceptibilities (see also Refs. 5 and 6). The other approximation, notably that with the entire term (13), will be used in subsequent papers.

III. LINEAR OPTICAL SUSCEPTIBILITY IN EXCITONIC AND VIBRONIC REGIONS

We perform the calculations of the linear optical susceptibility χ_{ij} using the expression:[1,7,10]

$$\chi_{ij} = \lim_{\epsilon \to 0} \left\{ -\frac{1}{2\hbar V} [\Phi_{ij}(\omega + i\epsilon) + \Phi_{ij}(-\omega + i\epsilon)] \right\}, \tag{26}$$

with

$$\Phi_{ij} = -i\theta(t)\langle 0 | P_i(t) P_j(0) + P_j(t) P_i(0) | 0 \rangle, \tag{27}$$

$$\hat{P} = \sum_n \hat{P}_n, \tag{28}$$

where $\hat{P}_n$ is the operator of the electric (transition) dipole moment of the excitons on site n. The Green function (27) has been calculated as average over the ground state $|0\rangle$ taking into account the large values of the energy of the excitons and vibrational quantum: E_F, E_c, $\hbar\omega_0 \gg \kappa T$. The operator

$$\hat{P}_1 = \sum_n \hat{P}_n = \sum_n \left[\mathbf{P}_F (B_n^+ + B_n) + \mathbf{P}_{CT} \times \frac{1}{\sqrt{2}} (C_{n1} + C_{n2} + C_{n1}^+ + C_{n2}^+) \right] \tag{29}$$

is transformed into the following operator:

$$\hat{P} = e^{Q} \hat{P}_1 e^{-Q} = \sum_{n,\sigma} [\mathbf{P}_F (V_n + V_n^+) + (\mathbf{P}_{CT}/\sqrt{2})(U_{n\sigma} + U_{n\sigma}^+)], \tag{30}$$

where $\mathbf{P}_F$ is the electric transition dipole of the Frenkel exciton, and $\mathbf{P}_{CT}$ is the electric transition dipole of the symmetrical CTE's state $(1/\sqrt{2})(C_{n1}^+ + C_{n2}^+)|0\rangle$ (the antisymmetrical combination $(1/\sqrt{2})(C_{n1}^+ - C_{n2}^+)|0\rangle$ does not mix with FE due to symmetry reasons[8,9]).

In this paper, we study the linear absorption spectra in the excitonic and one-phonon vibronic regions using the larger part of the transition dipoles (30) associated with Frenkel excitons only:[8,9,11]

$$\hat{P}_{FE} = \hat{P}_F e^{\delta_1} \sum_n [B_n + B_n^+ + f(B_n a_n + B_n^+ a_n^+)], \tag{31}$$

where

$$f = d_1/\cosh(2\tau) \tag{32}$$

(see Appendix B).

We calculate Green functions (27) using the standard procedure of differentiation with respect to time of the corresponding functions. The excitonic and one-phonon vibronic contributions to the linear susceptibility χ_{ij} can be expressed as follows:

$$\chi_{ij} = -\exp(2\delta_1) P_F^i P_F^j [G(k=0) + f^2 S_0(\omega)]. \tag{33}$$

The formula which yields the excitonic Green function $G(k=0)$, corresponding to the center $k=0$ of the Brillouin zone in momentum space, has the form:

$$G(k=0) = [\hbar\omega - E_F - 2L - 2(\varepsilon_e + \varepsilon_h)^2/(\hbar\omega - E_c)]^{-1}. \tag{34}$$

Function $S_0(\omega)$ in Eq. (33) expresses the contribution of the one-phonon vibronic spectrum to the linear susceptibility and the calculations performed with Hamiltonians (12) and (18) give the following result:

$$S_0(\omega) = \frac{1}{2LD} \left[\sigma(t) - \frac{\eta \sigma_1(t)}{1+\varepsilon_2} \right], \tag{35}$$

where

$$\sigma(t) = \frac{1}{N} \sum_k \frac{1}{t - \cos ka}, \quad \sigma_1(t) = t\sigma(t) - 1, \tag{36}$$

$$t = (\Omega - \Delta - 2\varepsilon_1)/[2(1+\varepsilon_2)], \tag{37}$$

$$\Omega = [\hbar(\omega - \omega_0) - E_c]/L, \tag{38}$$

$$\Delta = (E_F - E_c)/L, \tag{39}$$

$$\varepsilon_1 = (\varepsilon_{e1}^2 + \varepsilon_{h1}^2)/\Omega, \quad \varepsilon_2 = 2\varepsilon_{e1}\varepsilon_{h1}/\Omega, \tag{40}$$

$$\varepsilon_{e1} = \varepsilon_e/L, \quad \varepsilon_{h1} = \varepsilon_h/L, \tag{41}$$

$$D = 1 + \varepsilon_2 - \kappa\sigma(t) - \sigma_1(t)[2\lambda + \eta t + (\lambda^2 - \kappa\eta)/(1+\varepsilon_2)] - [\hbar\Delta\omega/(2L)][\sigma(t) - \eta\sigma_1(t)/(1+\varepsilon_2)], \tag{42}$$

$$\lambda = -\eta_1 + \varepsilon_1' \eta_3 [1 - \eta_2 + (1-\eta_4)e^{-2\tau}] + \varepsilon_2' [\eta_3^2 e^{-2\tau} + (1-\eta_2)(1-\eta_4)] - \varepsilon_2, \tag{43}$$

$$\kappa = \eta_1 e^{2\tau} + \varepsilon_1' [\eta_3^2 + (1-\eta_4)^2] - \varepsilon_1 + 2\varepsilon_2' \eta_3 (1-\eta_4), \tag{44}$$

$$\eta = \eta_1 e^{-2\tau} + \varepsilon_1' [\eta_3^2 e^{-4\tau} + (1-\eta_2)^2] - \varepsilon_1 + 2\varepsilon_2' \eta_3 (1-\eta_2), \tag{45}$$

$$\varepsilon_1' = (\varepsilon_{e1}^2 + \varepsilon_{h1}^2)/(\Omega - \hbar\Delta\omega^+/L), \tag{46}$$

$$\varepsilon_2' = 2\varepsilon_{e1}\varepsilon_{h1}/(\Omega - \hbar\Delta\omega^+/L).$$

Sum (36) spreads over all values of the wave number k in the Brillouin zone:

$$k = (0, \pm 1, \ldots, \pm N/2) 2\pi/(aN), \tag{47}$$

in which a is the distance between neighbor equivalent units in the stack. Sum (36) depends on the quantity Ω which can be presented as

$$\Omega = y_1 + i\delta, \tag{48}$$

where y_1 is a real quantity, and $i\delta$ is a small imaginary part that describes excitons' and phonons' damping. Notably the imaginary part $i\delta L$ yields the width of the excitonic and vibronic levels.

TABLE I. Exciton parameters for a MePTCDI crystal.

Quantity Z	E_F	E_c	$\Delta = E_F - E_c$	L	ε_e	ε_h	$\hbar\omega_0$
Value of Z (eV)	2.23	2.15	0.08	0.044	−0.047	−0.017	0.17
Value of Z/L			1.83	1	−1.07	−0.39	3.86

The vibronic spectrum consists of two well-known types of exciton–phonon states, namely:

(a) Many-particle (MP) states which correspond to values $|t|<1$ [see Eq. (37)]. In the nearest-neighbors approximation function $\sigma(t)$ takes the form:

$$\sigma(t)=\begin{cases}\dfrac{1}{\sqrt{t^2-1}}\ \mathrm{sgn}\ t_1, & |t_1|>1,\\ -\dfrac{i}{\sqrt{1-t^2}}\ \mathrm{sgn}[y^2+2\varepsilon_{e1}\varepsilon_{h1}(2y-\Delta)+2(\varepsilon_{e1}^2+\varepsilon_{h1}^2)], & |t_1|<1,\end{cases} \tag{49}$$

where

$$t_1=\frac{y^2-y\Delta-2(\varepsilon_{e1}^2+\varepsilon_{h1}^2)}{2(y+2\varepsilon_{e1}\varepsilon_{h1})}. \tag{50}$$

The values of $\Omega=y+i\delta$, which correspond to $|t_1|<1$, form two continua.

(b) Bound exciton–phonon states (BS). Their levels are the discrete poles ($|t_1|>1$) of the function $S_0(\omega)$ outside the above-mentioned MP continua.

IV. LINEAR ABSORPTION SPECTRA

In this section, we model the absorption spectra calculating the imaginary part of functions (34) and (35) in which the exciton parameters of the MePTCDI crystal[8] are introduced.

The unit cell of this crystal contains two nonequivalent molecules[3,8] that build two types A and B of one-dimensional stacks. We calculate, as in Ref. 1, the linear optical susceptibility in an oriented gas model. In this way, we neglect the possible transfer of FE and CTEs between the molecules of different stacks A and B, and, correspondingly, we ignore the Davydov splitting of the excitonic and vibronic spectra. The interstack transfer is beyond our basic Hamiltonian (1) and (2). We mention here another reason for our restriction on the oriented gas model. The intermolecular distance inside the stacks of perylene derivatives ($a\approx 3.5$ Å) is several times smaller than the distances between the molecules of different orientations which are located in a plane perpendicular to the stacks' axis. Thus the interstacks exciton transfer would be less probable than the transfer inside a stack.

Following Ref. 8, we define the FE plane on which transition dipoles $\mathbf{P}_F^A$ and $\mathbf{P}_F^B$ ($|\mathbf{P}_F^A|=|\mathbf{P}_F^B|=P_F$) are situated. The x axis coincides with the direction of the sum $\mathbf{P}_F^A+\mathbf{P}_F^B$, the y axis also is lying on the FE plane, and φ is the angle between the two transition dipoles ($\varphi=36.8°$, see Ref. 8).

The linear optical susceptibility of a crystal with N_2 pairs of stacks (A, B) can be represented as

$$\chi_{xx}=-Ae^{2\delta_1}[G(k=0)+f^2S_0(\omega)]\cos^2(\varphi/2), \tag{51a}$$

$$\chi_{yy}=-Ae^{2\delta_1}[G(k=0)+f^2S_0(\omega)]\sin^2(\varphi/2), \tag{51b}$$

where

$$A=2P_F^2NN_2/(VL). \tag{52}$$

We take the exciton parameters of the MePTCDI crystal according to Refs. 8 and 9 [see Table I, in which all quantities of interest (Z) are normalized with respect to L].

In the calculation of $\mathrm{Im}\{\chi_{xx}/[A\cos^2(\varphi/2)]\}$ we introduce the imaginary part of the dimensionless frequency (48), $\delta=0.01$, which corresponds to $L\delta$ as a proper width of the exciton and phonon lines.

A. Excitonic region

In calculating the excitonic absorption governed by the quantity $-\exp(2\delta_1)G(k=0)$, the parameters of exciton–phonon coupling enter the quantity δ_1 only and do not shift the position of excitonic maxima. Figures 1–12 contain the absorption curves calculated as the imaginary part of the function

$$\chi_{xx}/[A\cos^2(\varphi/2)]=-\exp(2\delta_1)[G(k=0)+f^2S_0(\omega)]. \tag{53}$$

Two Lorentzian maxima appear at the frequencies of the poles of function (34). The repulsion of the levels caused by the FE–CTEs mixing and expressed through charge-transfer integrals ε_e and ε_h shifts the absorption peaks which can be assigned as renormalized CTEs levels $\hbar\omega_{CTEs}=2.110$ eV and a FE level $\hbar\omega_{FE}=2.358$ eV.

The different values of the parameters of exciton–phonon coupling can change the magnitudes of the excitonic maxima (but not their position).

B. One-phonon vibronic region

The vibronic spectrum is governed by the quantity $-\exp(2\delta_1)f^2S_0(\omega)$ and strongly depends on the parameters d, d^+, e, e^+ of the exciton–phonon coupling. Direct data for the linear and quadratic exciton–phonon coupling are not available and thus we model the vibronic spectra using various sets of parameters.

We introduce the following values for the parameter d of FE–vibration coupling: (i) $d=1$ that corresponds to an intermediate linear coupling; (ii) $d=0.8$ describing a weak coupling (but close to the probable values for a molecule in a MePTCDI crystal); and (iii) $d=1.2$ which models a relatively strong coupling.

The magnitudes of the parameter e of quadratic coupling are correlated with the relative frequency shift $\Delta\omega/\omega_0$ of the

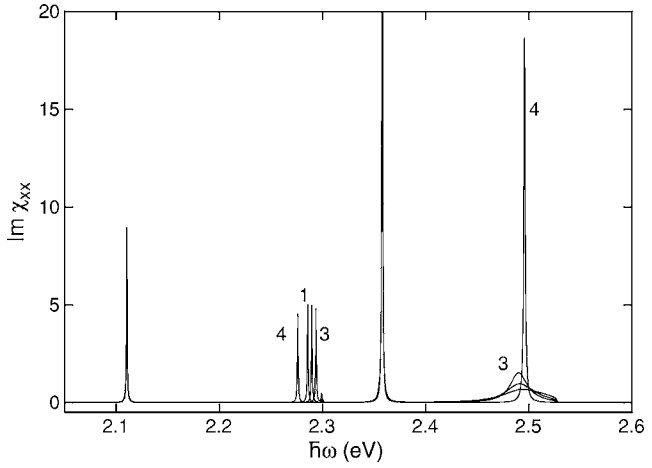

FIG. 1. Linear absorption spectra of the MePTCDI crystal (see the exciton parameters in Table I). The values of the parameters of exciton–phonon coupling are $d^+=d=0.8$, $e^+=e$. For curve 1 $e=-0.015$, curve 2 $e=0$, curve 3 $e=+0.015$, and for curve 4 $e=-0.05$. The absorption lines at $\hbar\omega=2.110$ and 2.358 eV correspond to pure excitonic absorption of mixed FE+CTEs. The two vibronic replicas are positioned near $\hbar\omega\approx 2.3$ and 2.5 eV, respectively.

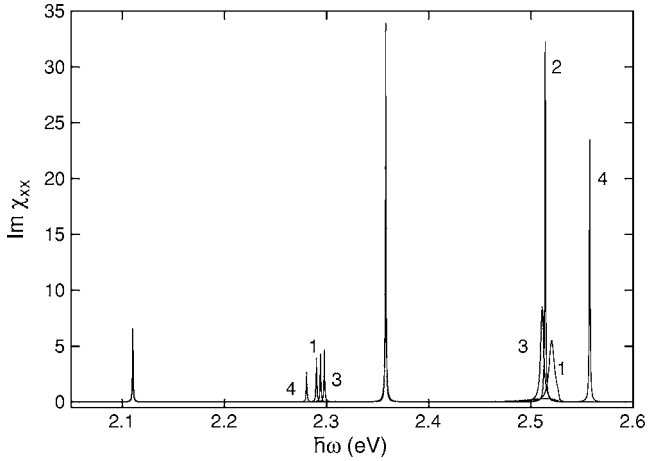

FIG. 2. The same as Fig. 1 with $d^+=d=1$ (intermediate case).

vibration in an electronically excited molecule. According to formula (14c),

$$\Delta\omega/\omega_0 \approx 2e, \quad |e| \ll 1. \tag{54}$$

For the crystal under consideration the most probable are small relative shifts, $\Delta\omega/\omega_0\approx -0.01$ (or even smaller). We illustrate the role of the quadratic coupling by taking the following values: (i) $e=-0.015$; (ii) $e=0$; (iii) $e=+0.015$; and (iv) $e=-0.05$. A positive value of e is a rather curious case.

The probable values of the parameters for the exciton–phonon coupling in the ions of the MePTCDI crystal [the parameters for positive and negative ions have been assumed to be equal, see Eq. (15)] are supposed to be as follows:

(1) $d^+=d$, as a simple case (see Ref. 3);

(2) $d^+=d/\sqrt{2}$ (see Refs. 3 and 4)—in this case the vibrational relaxation energy $d^2\hbar\omega_0$ of the Frenkel exciton and that of the CTE $[(d^+)^2+(d^-)^2]\hbar\omega_0$ are equal;

(3) $e^+=e$, again an even simpler case; and

(4) $e^+=2e$, supposing a more stronger change of the vibrational frequency in ions than in the neutral electronically excited molecule.

1. Case $d^+=d$

The one-phonon vibronic lines are positioned near $\hbar\omega\approx 2.3$ eV and around $\hbar\omega\approx 2.5$ to 2.6 eV. The combination of CTEs excitonic line $\hbar\omega=2.110$ eV and the spectral structures near $\hbar\omega\approx 2.3$ eV creates an excitonic and first vibronic replica of CTEs whereas the combination of the FE line $\hbar\omega=2.358$ eV and the structures near and above $\hbar\omega=2.5$ eV can be treated as a FE and its first vibronic. We stress again on the necessity of a very careful assignment of the absorption lines (see Ref. 1).

In the case of weak exciton–phonon coupling, $d^+=d=0.8$ (Fig. 1), the vibronics of CTEs near 2.3 eV form nonintensive and narrow Lorentzian curves. The quadratic exciton–phonon coupling, $e^+=e$, shifts their positions to the lower energies ($e<0$) or in opposite direction at $e>0$. A weak upper component of absorption line near 2.3 eV would be practically nonobservable. The vibronics of FE near $\hbar\omega\approx 2.5$ eV create a wide and flat absorption maximum of bigger integral intensity than the maxima of CTEs vibronics. It corresponds to the excitation of two unbound quasiparticles—one exciton and one phonon—and the sum of their energies forms a relatively wide continuum called *many-particle band* (MP). Irrespective of its big spectral density, the absorption line would be structureless and very wide. We note two other details.

(a) The vibronic lines of CTEs near 2.3 eV describe the *bound state* (BS) of the CTE and the vibrational quantum. The spectral width of the bound states' lines is equal to the width of the excitonic lines (in our calculations it is very close to the quantity $L\delta$).

(b) The stronger quadratic coupling $e=-0.05$, which corresponds to a relative frequency change $\Delta\omega/\omega_0\approx -0.1$ in the excited molecule, modulates very strongly the vibronic absorption in the MP continuum near 2.5 eV. The absorption line is narrowed and it describes a quasibound exciton–phonon state (see curve 4 in Fig. 1).

The intermediate linear coupling, $d^+=d=1$ (Fig. 2), was called the *molecular vibron case*.[4,8] In the absence of quadratic coupling the absorption is caused by nonseparable bound exciton–phonon states and two Lorentzian maxima appear at $e=0$ (see curve 2 in Fig. 2) as vibronics of CTEs and FE. The quadratic coupling shifts the position of the CTEs vibronic line near 2.3 eV but does not change its shape. However, even a small quadratic coupling, $e=\pm 0.015$ destroys the molecular vibron state near 2.5 eV. Figure 2 illustrates the possible drastic change in the line shape depending on the sign of e. In the case of $d^+=d=1$ and stronger quadratic coupling, $e=-0.05$ (curve 4 in Fig. 2), a bound state above the MP continuum concentrates the absorption intensity near $\hbar\omega=2.56$ eV.

In the case of strong linear exciton–phonon coupling (Fig. 3) the vibronic absorption in both regions $\hbar\omega\approx 2.3$ eV (vi-

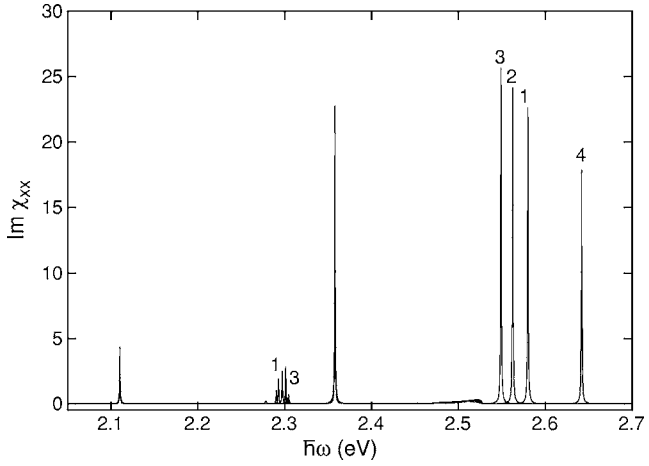

FIG. 3. The same as Fig. 1 with $d^+=d=1.2$ (strong coupling).

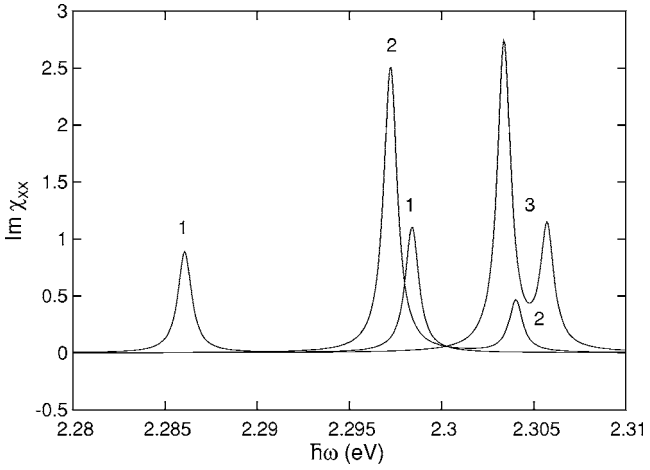

FIG. 5. The same as Fig. 4 with $d^+=d=1.2$, $e^+=2e$.

bronics of CTEs) and $\hbar\omega\approx 2.5$–2.7 eV (vibronics of FE) consists of Lorentzian maxima and exhibits predominantly bound states. The quadratic coupling shifts the vibronic lines of CTEs and FE in opposite directions. Obviously the shifting of the FE vibronic line near $\hbar\omega\approx 2.6$ eV is rather bigger than the shifting of the CTEs vibronic line near 2.3 eV.

Figures 4 and 5 illustrate the case $d^+=d$ and $e^+=2e$. The larger quadratic coupling in ions changes the quantity $\Delta\omega^+$ [see Eq. (14c)] which enters quantities (46) through the difference

$$\Omega - \hbar\,\Delta\omega^+/L = [\hbar(\omega-\omega_0) - E_c - \hbar\,\Delta\omega^+]/L. \qquad (55)$$

Since the value $\hbar\omega_0+E_c=2.32$ eV is much closer to the CTEs vibronic line at $\hbar\omega\approx 2.3$ eV than to the FE vibronic line around $\hbar\omega\approx 2.5$–2.7 eV, even small values of $\Delta\omega^+$ shift the position of CTEs vibronic and do not influence the position of the FE vibronic line. The most sensitive change of the absorption line near 2.3 eV in Fig. 4 is the appearance of a spectral doublet at $e=+0.0015$. The splitting of the doublet's components is $\Delta_1\approx 0.005$ eV. This value corresponds very well to the quantity

$$\hbar\,\omega_0(2e^+ - 2e) \approx \hbar\,\Delta\omega^+ - \hbar\,\Delta\omega$$

at $e^+=2e=0.03$. So, two types of bound exciton–phonon states can be observed in this case: (i) the vibrational quantum is excited on ions, and (ii) the vibrational quantum exists on the neutral molecule which is electronically excited (the lower component of the doublet near 2.3 eV). The case of strong coupling (Fig. 5) illustrates the appearance of similar doublets in the absorption near 2.3 eV (at $e\neq 0$), but not near the vibronic structure of FE above 2.5 eV, where the absorption spectra are very close to those in Fig. 3.

2. Case $d^+=d/\sqrt{2}$

This assumption makes the calculations of absorption spectra more complicated [see Eqs. (20)–(22), (42)–(45)], but the general structure of the spectra is preserved.

The case of weak exciton–phonon coupling (Fig. 6) exhibits the same spectral structures as Fig. 1. The vibronic replica of FE is positioned in the MP continuum and the

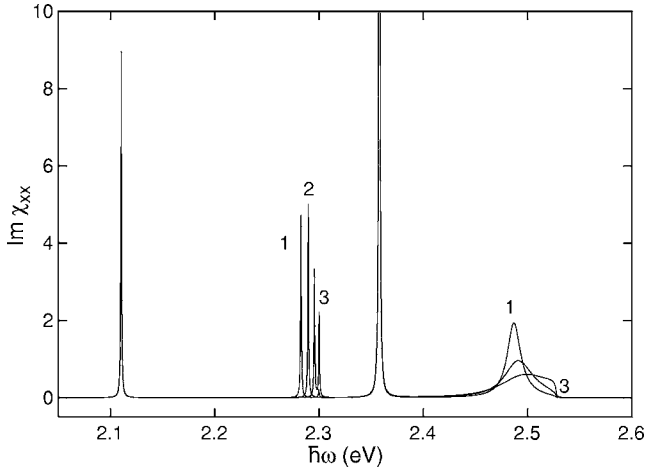

FIG. 4. Linear absorption spectra with $d^+=d=0.8$, $e^+=2e$. For curve 1 $e=-0.015$, curve 2 $e=0$, curve 3 $e=+0.015$.

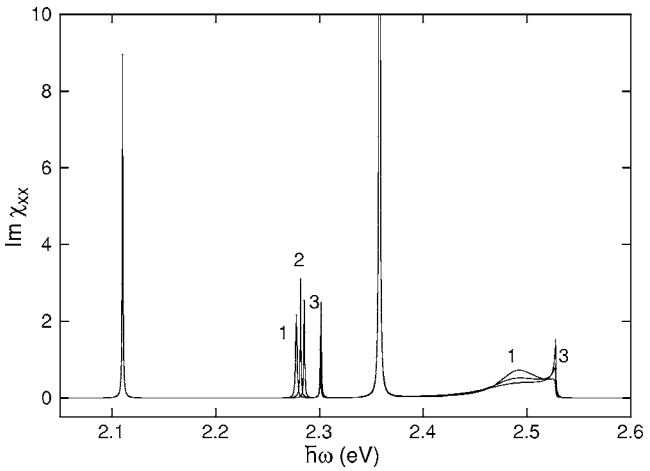

FIG. 6. Linear absorption spectra with $d=0.8$, $d^+=d/\sqrt{2}$, $e^+=e$. For curve 1 $e=-0.015$, curve 2 $e=0$, and curve 3 $e=+0.015$.

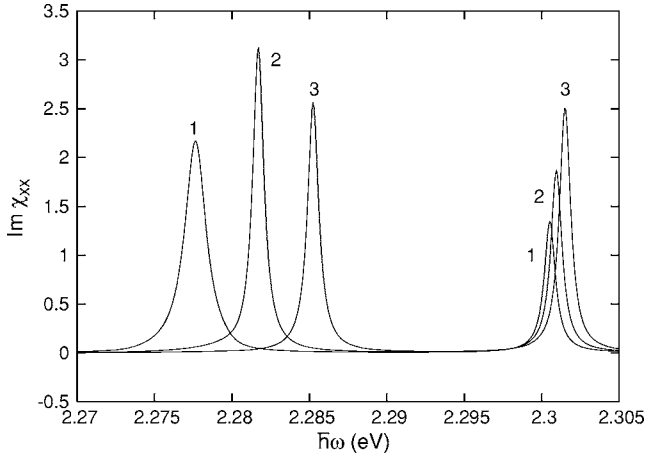

FIG. 7. Linear absorption spectra of CTEs' vibronics. For the other spectra see Fig. 6.

quadratic coupling can modulate its shape (see curve 3 in Fig. 6). Two components of the doublets near 2.3 eV have comparable intensities (Fig. 7). The position of the higher components depends very weakly on the quadratic coupling whereas the lower component is shifted with different values of the parameter of quadratic coupling e.

The intermediate coupling (Fig. 8) causes similar absorption. But the simultaneous action of the linear and quadratic coupling binds the exciton and phonon at $e=-0.015$ and the narrow and intensive maximum near 2.52 eV can be observed as a demonstration of the quasibound state.

The strong coupling (Fig. 9) creates intensive bound exciton–phonon states and the absorption spectra are close to those in Fig. 3. The doublet near 2.3 eV possesses two nonequal components.

Figures 10 and 11 illustrate the possible differences in absorption spectra caused by a two-times increasing of the quadratic coupling parameter e^+ (compare curves 1 and 2 in Fig. 10, the other parameters of the exciton–phonon coupling preserve their values). Whereas the absorption near $\hbar\omega \approx 2.5$ eV remains nonchanged, the doublets near $\hbar\omega \approx 2.3$ eV slightly shift their positions. As a general conclusion we can estimate the impact of e^+ on absorption as a relatively weak one.

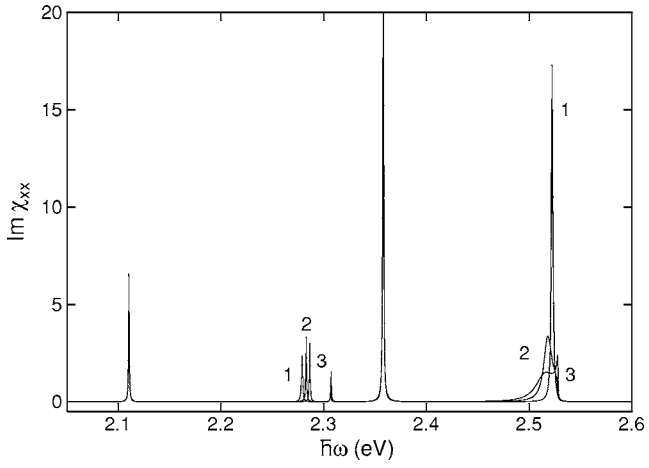

FIG. 8. The same as Fig. 6 with $d=1$.

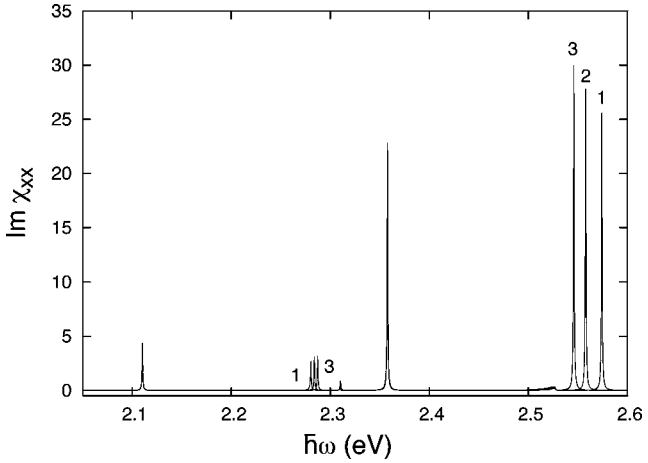

FIG. 9. The same as Fig. 6 with $d=1.2$.

The stronger impact of various values of the constant for linear coupling $d^+=d$ and $d^+=d/\sqrt{2}$ is illustrated in Fig. 12. The absorption near 2.3 eV exhibits a single Lorentzian maximum at $d^+=d$; in the case of $d^+=d/\sqrt{2}$ it splits into two maxima. The MP continuum near 2.5 eV is modulated and it has quite a different shape and maximal values of the absorption lines in these two cases.

3. Case $\Delta<0$

We turn now to a hypothetical case of reversed order of the levels of FE and CTEs. We put the same values of all other quantities as in the previous calculations except the value of E_F (see Table I). We suppose that $E_F=2.07$ eV, and hence $\Delta=-0.08$ eV. This case does not follow the original parametrization of the excitons in the MePTCDI crystal (see Refs. 8 and 9) and may be available for other crystals with a different sequence of the excitonic levels.

The absorption spectra represented in Figs. 13–15 show the position of pure excitonic levels at $\hbar\omega=2.065$ eV and $\hbar\omega=2.246$ eV. The mixing of FE and CTEs is stronger than the corresponding mixing at $\Delta>0$ and thus these two absorption maxima possess nearly equal intensities.

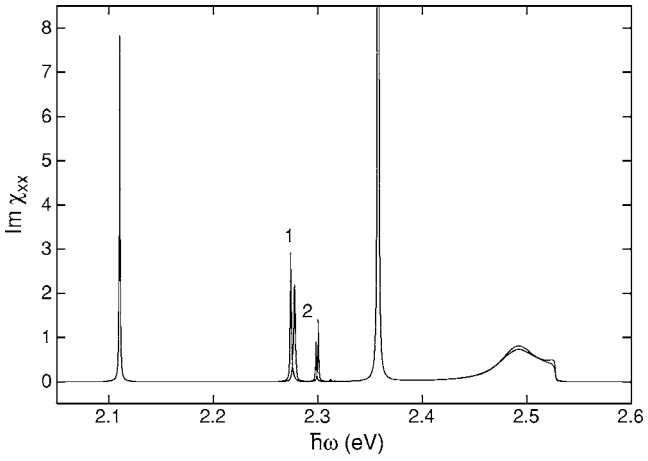

FIG. 10. Linear absorption with $d=0.8$, $d^+=d/\sqrt{2}$, $e=-0.015$. For curve 1 $e^+=e$, curve 2 $e^+=2e$.

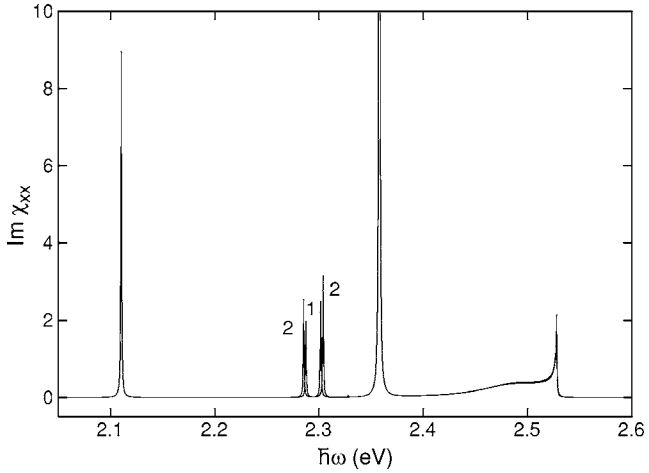

FIG. 11. The same as Fig. 10 with $e=+0.015$.

The other structures in the absorption spectra in Figs. 13–15 correspond to one-phonon vibronics and their manifestation is similar to the case of $\Delta>0$ (Figs. 1–12). In the case $\Delta<0$, the vibronic doublet near $\hbar\omega\approx 2.25$ eV is positioned in the same spectral region as the absorption maximum of the mixed excitons FE+CTEs. The splitting of the two components of the doublet is better expressed in the case $d^+=d/\sqrt{2}$. The splitting and intensity of the doublet are bigger in the case $\Delta<0$ than in the opposite case $\Delta>0$. An MP band appears near $\hbar\omega\approx 2.4$ eV (see Figs. 13 and 14) which is the analog of the MP band near $\hbar\omega\approx 2.5$ eV in Figs. 1, 2, 6, and 8. In the case of strong exciton–phonon coupling (Fig. 15) an intensive Lorentzian maximum appears above that band as a demonstration of the bound exciton–phonon state.

V. CONCLUSIONS

In this paper, we have investigated the excitonic and vibronic spectra of mixed Frenkel and charge-transfer excitons. We used the model and exciton parameters of the MePTCDI crystal having the intention to obtain more general results on the structure as well as a demonstration of excitons and vibronics in other subjects, too. The studies of excitons via the linear absorption and excitonic photoluminescence[12–15] confirm the necessity of a detailed knowledge of the coupling between FE and CTEs and their vibronic satellites. Thus the simultaneous treatment of linear and quadratic exciton–phonon coupling can be important from a theoretical point of view and in the interpretation of the spectra of other crystals as well.

We consider as the most interesting conclusions the following.

1. The vibronics of mixed FE and CTEs create two spectral structures and the corresponding frequency regions are relatively separated. We can consider, not in absolute meaning, as two separate combinations the excitonic line of CTEs and their first vibronic, and on the other hand, the excitonic line of the FE and its vibronic.

2. The vibronics of CTEs form a spectral doublet of narrow Lorentzian maxima associated with two transferring mechanisms, notably the hoppings of CTE's electron and hole. This doublet structure is clearly expressed in the case

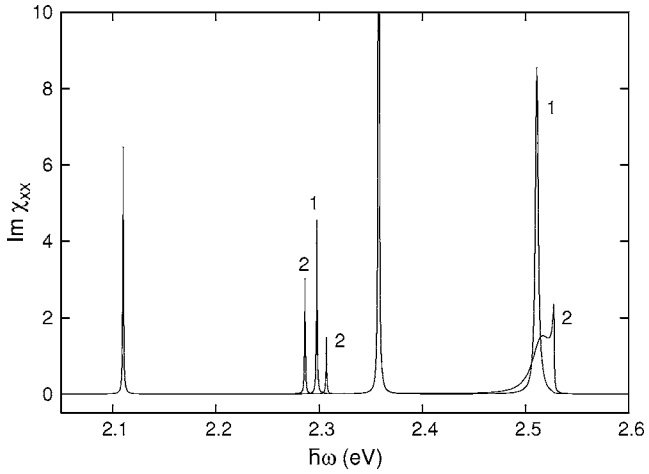

FIG. 12. Linear absorption with $d=1$, $e^+=e=-0.015$. For curve 1 $d^+=d$, curve 2 $d^+=d/\sqrt{2}$.

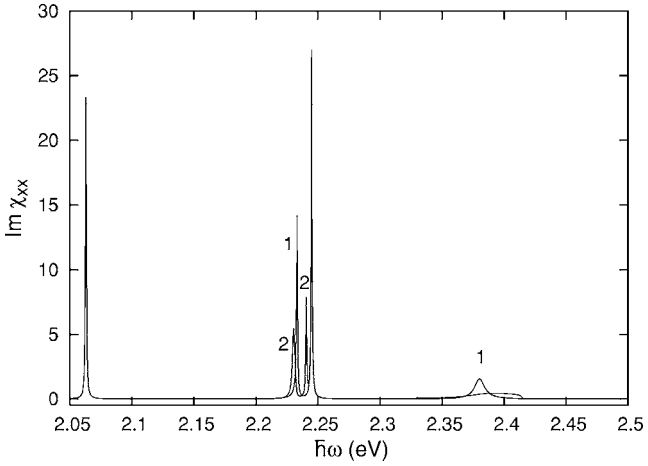

FIG. 13. Absorption spectra at $E_c=2.15$ eV, $E_F=2.07$ eV with $d=0.8$, $e^+=e=-0.015$. For curve 1 $d^+=d$, while for curve 2 $d^+=d/\sqrt{2}$. The absorption maxima $\hbar\omega=2.065$ and 2.246 eV correspond to pure excitonic levels.

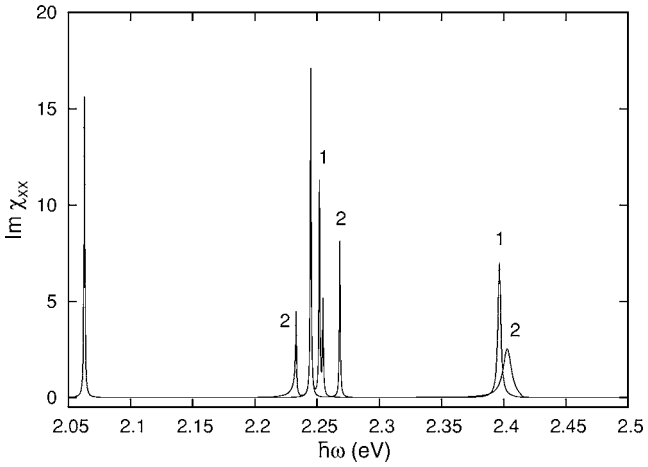

FIG. 14. The same as Fig. 13 with $d=1$.

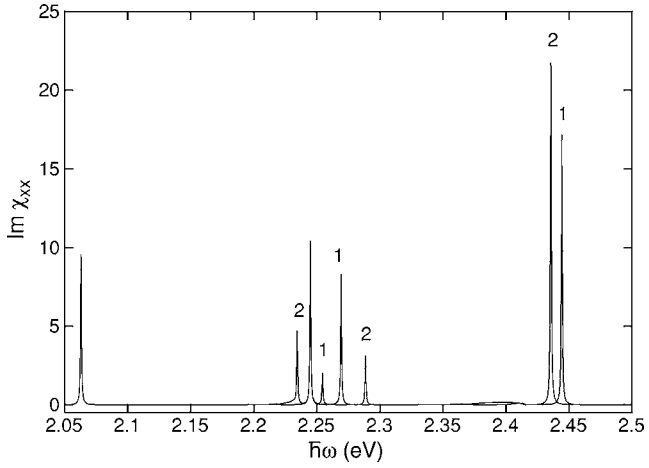

FIG. 15. The same as Fig. 13 with $d=1.2$.

of nonequal values of the parameters of FE–phonon and CTEs–phonon couplings [$d^+ \neq d$ and $e^+ \neq e$ in Eqs. (5)].

3. We establish the stronger impact of the linear exciton–phonon coupling on the linear absorption compared with the influence of the quadratic coupling.

4. In the case of weak linear coupling, in the model of excitons in a MePTCDI crystal, the vibronics of FE create a wide and flat absorption line appearing in the continuum of the MP states. But a strong quadratic coupling could narrow the vibronic line of FE. In the case of weak linear exciton–phonon coupling the vibronics of FE and CTEs manifest comparable intensities in the linear absorption.

5. In the case of intermediate linear coupling, $|d|=1$, the quadratic coupling can change drastically the line shapes of vibronics of FE which would be no longer narrow Lorentzian maxima (as it is at $e^+=e=0$, see Ref. 1) rather than becoming wide and flat continua. However, a strong quadratic coupling can create a Lorentzian maximum above those continua (see Fig. 2).

6. In the case of strong linear coupling ($|d|>1$) the vibronic's linear absorption exhibits predominantly bound exciton–phonon states. The position of narrow absorption maxima depends strongly on the parameters of quadratic exciton–phonon coupling which shifts the vibronic levels of CTEs and FE in opposite directions. In this case, the absorption intensity of the FE vibronics is considerably bigger than the intensity of CTEs vibronics.

The knowledge of the structure and details of vibronic spectra of molecular crystals can be very useful in estimating the parameters of exciton–phonon coupling—both linear and quadratic—which govern the linear absorption as well as the nonlinear optical properties of these promising for the organic electronics materials.

APPENDIX A

We find the following operator relation:

$$F(\tau) = \exp\{\tau[a^2 - a^{+2} + \theta(a - a^+)]\}$$
$$= \exp(\alpha_1 a^{+2})\exp(\alpha_2 a^+)\exp(\alpha_3 a^+ a)\exp(\alpha_4 a) \times \exp(\alpha_5 a^2)\exp(\delta), \quad \text{(A1)}$$

where a and a^+ are boson annihilation and creation operators, τ is a scalar argument, θ is a numerical parameter, and α_i $(i=1-5)$, δ are the following scalar functions of τ:

$$\alpha_1 = -\alpha_5 = -(1/2)\tanh(2\tau), \quad \text{(A2)}$$

$$\alpha_2 = \frac{\theta}{2}\frac{1-\exp(2\tau)}{\cosh(2\tau)}, \quad \text{(A3)}$$

$$\alpha_4 = \frac{\theta}{2}\frac{1-\exp(-2\tau)}{\cosh(2\tau)}, \quad \text{(A4)}$$

$$\alpha_3 = -\ln\cosh(2\tau), \quad \text{(A5)}$$

$$\exp(\delta) = \frac{1}{\sqrt{\cosh(2\tau)}}\exp[(1/4)\theta^2(1/\cosh(2\tau)-1)]. \quad \text{(A6)}$$

The differentiation of Eq. (A1) with respect to τ yields

$$\frac{dF}{d\tau} = F[a^2 - a^{+2} + \theta(a-a^+)]$$
$$= \frac{d\alpha_1}{d\tau}\exp(\alpha_1 a^{+2})a^{+2}\exp(\alpha_2 a^+)\exp(\alpha_3 a^+ a)\cdots$$
$$+ \frac{d\alpha_2}{d\tau}\exp(\alpha_1 a^{+2})\exp(\alpha_2 a^+)a^+\exp(\alpha_3 a^+ a)\exp(\alpha_4 a)\cdots \quad \text{(A7)}$$

[the other terms with the derivatives $d\alpha_3/d\tau$, $d\alpha_4/d\tau$, $d\alpha_5/d\tau$, $d\delta/d\tau$ are similar to the first two terms on the right-hand side of Eq. (A7)].

It is easy to establish the following commutative relations:

$$a^+\exp(\beta a) = \exp(\beta a)(a^+ - \beta), \quad \text{(A8)}$$

$$a^+\exp(\alpha a^2) = \exp(\alpha a^2)(a^+ - 2\alpha a), \quad \text{(A9)}$$

$$a^+\exp(\alpha a^+ a) = \exp(-\alpha)\exp(\alpha a^+ a)a^+ \quad \text{(A10)}$$

and their Hermitian analogs. Using these relations we obtain a set of six differential equations which contain six unknown functions α_i, δ and their derivatives. We write down here three equations:

$$(d\alpha_1/d\tau)\exp(-2\alpha_3) = -1, \quad \text{(A11)}$$

$$-4\alpha_5^2 - 2\alpha_5(d\alpha_3/d\tau) + d\alpha_5/d\tau = 1, \quad \text{(A12)}$$

$$d\alpha_3/d\tau = -4\alpha_5. \quad \text{(A13)}$$

Their solutions [see Eqs. (A2)–(A6)] vanish at $\tau=0$ since $F(0)=1$.

APPENDIX B

We take into account relations (7) and (8) and find the following expressions:

$$e^{Q} = 1 + \sum_{n} B_n^{+} B_n [\exp(\tau\beta_n) - 1] + \sum_{n,\sigma=1,2} C_{n\sigma}^{+} C_{n\sigma} [\exp(\tau_1 \alpha_{1n}) \exp(\tau_1 \alpha_{2,n+\sigma_1}) - 1], \tag{B1}$$

where

$$\beta_n = a_n^2 - a_n^{+2} + \theta(a_n - a_n^{+}), \tag{B2}$$

$$\alpha_{i,n} = a_n^2 - a_n^{+2} + \theta_i(a_n - a_n^{+}), \quad i = 1,2. \tag{B3}$$

The operators $b_{n_1}^{+}$ and b_{n_1} listed below appear as a result of the canonical transformation (6):

$$b_{n_1}^{+} = e^{Q} a_{n_1}^{+} e^{-Q}, \quad b_{n_1} = e^{Q} a_{n_1} e^{-Q}. \tag{B4}$$

On using commutative relations (A8)–(A10), relations (8) which are valid in the linear case with one exciton only, and relation (A1), we obtain the following expressions (see Ref. 5 for the case of vibronics of pure Frenkel excitons):

$$\begin{aligned} b_{n_1} = {} & a_{n_1} + B_{n_1}^{+} B_{n_1} \{ a_{n_1} [\cosh(2\tau) - 1] + a_{n_1}^{+} \sinh(2\tau) + (\theta/2) \\ & \times [\exp(2\tau) - 1] \} + (C_{n_1,1}^{+} C_{n_1,1} + C_{n_1,2}^{+} C_{n_1,2}) \\ & \times \{ a_{n_1} [\cosh(2\tau_1) - 1] + a_{n_1}^{+} \sinh(2\tau_1) + (\theta_1/2) \\ & \times [\exp(2\tau_1) - 1] \} + (C_{n_1-1,1}^{+} C_{n_1-1,1} + C_{n_1+1,2}^{+} C_{n_1+1,2}) \\ & \times \{ a_{n_1} [\cosh(2\tau_2) - 1] + a_{n_1}^{+} \sinh(2\tau_2) + (\theta_2/2) \\ & \times [\exp(2\tau_2) - 1] \} \end{aligned} \tag{B5}$$

(plus its Hermitian conjugated relation for $b_{n_1}^{+}$).

Now we express the phonon normal coordinate X_n [see Eq. (4)] and operators (5) of exciton–phonon coupling, as well as the phonon part (3) via operators b_{n_1} and $b_{n_1}^{+}$. Then the problem of elimination of operators (5) is reduced to three independent subproblems, namely: elimination of operator (5a) of exciton–phonon coupling in a molecule with FE, elimination of operator (5b) of exciton–phonon coupling in a positive ion, and finally, elimination of (5c) which concerns a negative ion. The proper choice of the parameters τ, τ_1, τ_2, θ, θ_1, and θ_2 [see relations (10) and (11)] simplifies the exciton–phonon part of the Hamiltonian (12).

Operator (13) which describes FE and CTEs transfer can be transformed by preserving these terms only in the expansion of the exponent's operator $\exp Q$ which contains one operator of creation and one operator of annihilation of the vibrational quantum. Notably this part of operator (13) of exciton transfer commutates with the operator (17) of total phonon numbers and it is the most essential for the one-phonon vibronic spectra.

In the linear case with small excitons' density the excitonic operators B_n, B_n^{+}, $C_{n\sigma}$, $C_{n\sigma}^{+}$ fulfill the commutative relations for boson operators. Thus we use expression (B1) and commutative relation (A10) and find the following expressions:

$$V_n = e^{Q} B_n e^{-Q} = B_n \exp(-\tau\beta_n), \tag{B6}$$

$$U_{n\sigma} = e^{Q} C_{n\sigma} e^{-Q} = C_{n\sigma} \exp[-(\tau_1 \alpha_{1,n} + \tau_2 \alpha_{2,n+\sigma_1})] \tag{B7}$$

(plus their Hermitian analogs). The exponents in Eqs. (B6) and (B7) can be presented by using relation (A1) and expanding them up to the terms linear with respect to the phonon operators a_n and a_n^{+}. In this way we obtain

$$V_n \approx B_n e^{\delta} [1 + \alpha_2(-\tau) a_n^{+}][1 + \alpha_4(-\tau) a_n], \tag{B8}$$

$$V_n^{+} \approx B_n^{+} e^{\delta} [1 + \alpha_2(\tau) a_n^{+}][1 + \alpha_4(\tau) a_n], \tag{B9}$$

as well as similar expressions for the CTEs' operators $U_{n\sigma}$ and $U_{n\sigma}^{+}$. We put Eqs. (B8) and (B9) (and the similar formulas for $U_{n\sigma}$ and $U_{n\sigma}^{+}$) in the operator (13) of exciton transfer according to the rule to preserve the terms with one phonon creation and one phonon annihilation operator. In such a way, after some algebraic transformations, one obtains the operator (18).

[1] I. J. Lalov and I. Zhelyazkov, Chem. Phys. **321**, 223 (2006).
[2] A. Brillante and M. R. Philpot, J. Chem. Phys. **72**, 4019 (1980).
[3] M. H. Hennessy, Z. G. Soos, R. A. Pascal, Jr., and A. Girlando, Chem. Phys. **245**, 199 (1999).
[4] M. Hoffmann and Z. G. Soos, Phys. Rev. B **66**, 024305 (2002).
[5] E. I. Rashba, Zh. Eksp. Teor. Fiz. **50**, 1069 (1966) [Sov. Phys. JETP **23**, 708 (1966)]; Zh. Eksp. Teor. Fiz. **54**, 542 (1968) [Sov. Phys. JETP **27**, 292 (1968)].
[6] A. S. Davydov and A. A. Serikov, Phys. Status Solidi B **44**, 127 (1971).
[7] I. J. Lalov, C. Supritz, and P. Reineker, Chem. Phys. **309**, 189 (2005).
[8] M. Hoffmann, K. Schmidt, T. Fritz, T. Hasche, V. M. Agranovich, and K. Leo, Chem. Phys. **258**, 73 (2000).
[9] K. Schmidt, K. Leo, and V. M. Agranovich, in *Organic Nanostructures: Science and Applications*, edited by V. M. Agranovich and G. C. La Rocca (IOS Press, Amsterdam, 2002), p. 521.
[10] V. M. Agranovich, in *Spectroscopy and Exciton Dynamics of Condensed Molecular Systems*, edited by V. M. Agranovich and R. M. Hochstrasser (North-Holland, Amsterdam, 1983), p. 83.
[11] M. Hoffmann, Z. G. Soos, and K. Leo, Nonlinear Opt. **29**, 227 (2002).
[12] G. Mazur, P. Petelenz, and M. Slawik, J. Chem. Phys. **118**, 1423 (2003).
[13] I. Vragovic and R. Scholz, Phys. Rev. B **68**, 155202 (2003).
[14] A. Yu. Kobitski, R. Scholz, D. R. T. Zahn, and H. P. Wagner, Phys. Rev. B **68**, 155201 (2003).
[15] H. P. Wagner, A. De Silva, and T. U. Kampen, Phys. Rev. B **70**, 235201 (2004).